J Fluoresc (2014) 24:1603–1611
DOI 10.1007/s10895-014-1446-4

ORIGINAL PAPER

Radiative and Nonradioactive Electron Transfer in Donor–Acceptor Phenanthrimidazoles

J. Jayabharathi · V. Thanikachalam · P. Ramanathan · A. Arunpandiyan

Received: 27 June 2014 / Accepted: 20 August 2014 / Published online: 7 September 2014

Abstract Photoinduced electron transfer in a series of naphthyl substituted phenanthrimidazoles has been studied in solutions. The intramolecular charge transfer (CT) leads to a large Stokes shift and large dipole moment in the fluorescent state. Solvatochromic effects on the spectral position and profile of the stationary fluorescence spectra clearly indicate the CT character of the emitting singlet states of all the compounds studied. An analysis of the CT fluorescence lead to the quantities relevant for the electron transfer in the Marcus inverted region.

Keywords Intramolecular charge transfer · Marcus inverted region · Electronic coupling

Introduction

The intramolecular charge transfer (CT) absorption ($^1CT \leftarrow S_0$), radiative and radiationless charge recombination (CR) processes ($^1CT \rightarrow S_0$) have been explained by photoinduced electron transfer (ET) processes [1–5]. Mulliken and Murrell models of molecular CT complexes lead the analysis of rate of radiative ET processes [6–8] and also define the molecular conformation of the states involved in the excited-state ET process [9–13]. The large values of the electronic transition dipole moments (M_{flu}) of CT fluorescence implies the non orthogonal geometry of the donor (D) and acceptor (A) subunits in the lowest excited ^1CT states. The 9-anthryl and 9-acridyl derivatives of aromatic amine show the dependence of electronic structure and conformation of fluorescent ^1CT state on solvation [14, 15]. In low polar media the interactions between ^1CT state and locally excited (LE) states exist in a more planar conformation of D and A moieties than that in the ground state. In more polar solvents the strong solute-solvent interactions restrict the flattening of the excited D-A system and its conformation is same as that in the ground state. Proton– and charge-transfer reactions are the common processes involved in chemical reactions as well as in living systems [16–21]. The appropriate values of the electronic coupling elements are mainly determined by the interactions between the atoms forming the bond A–D can be theoretically predicted following the formalism proposed by Dogonadze et al. [22, 23]. Neglecting contributions from the σ orbitals, one can obtain for π-electronic systems

$$V_0 = C^A_{LUMO} C^D_{HOMO} \beta_{AD} \cos(\theta_{A\text{-}D}) + \text{cons.}, \quad (1)$$

$$V^A_{1,3} = C^A_{HOMO} C^D_{HOMO} \beta_{AD} \cos(\theta_{A\text{-}D}) + \text{cons.}, \quad (2)$$

$$V^D_{1,3} = C^A_{LUMO} C^D_{LUMO} \beta_{AD} \cos(\theta_{A\text{-}D}) + \text{cons.}, \quad (3)$$

where $\theta_{A\text{-}D}$ denotes the angle between the planes of the acceptor and donor subunits and C_{HOMO} and C_{LUMO} are the LCAO coefficients (as obtained for the individual chromophores) of the $2p_Z$ atomic orbitals (where z is the axis perpendicular to the acceptor or donor rings) of the highest occupied molecular orbital (HOMO) and of the lowest unoccupied molecular orbital (LUMO) located on the atoms forming the A–D bond. β is the resonance integral for these AD atoms and const. is

J. Jayabharathi (✉) · V. Thanikachalam · P. Ramanathan · A. Arunpandiyan
Department of Chemistry, Annamalai University, Annamalainagar 608 002, Tamilnadu, India
e-mail: jtchalam2005@yahoo.co.in

Scheme 1 Mechanistic way for the synthesis of imidazoles

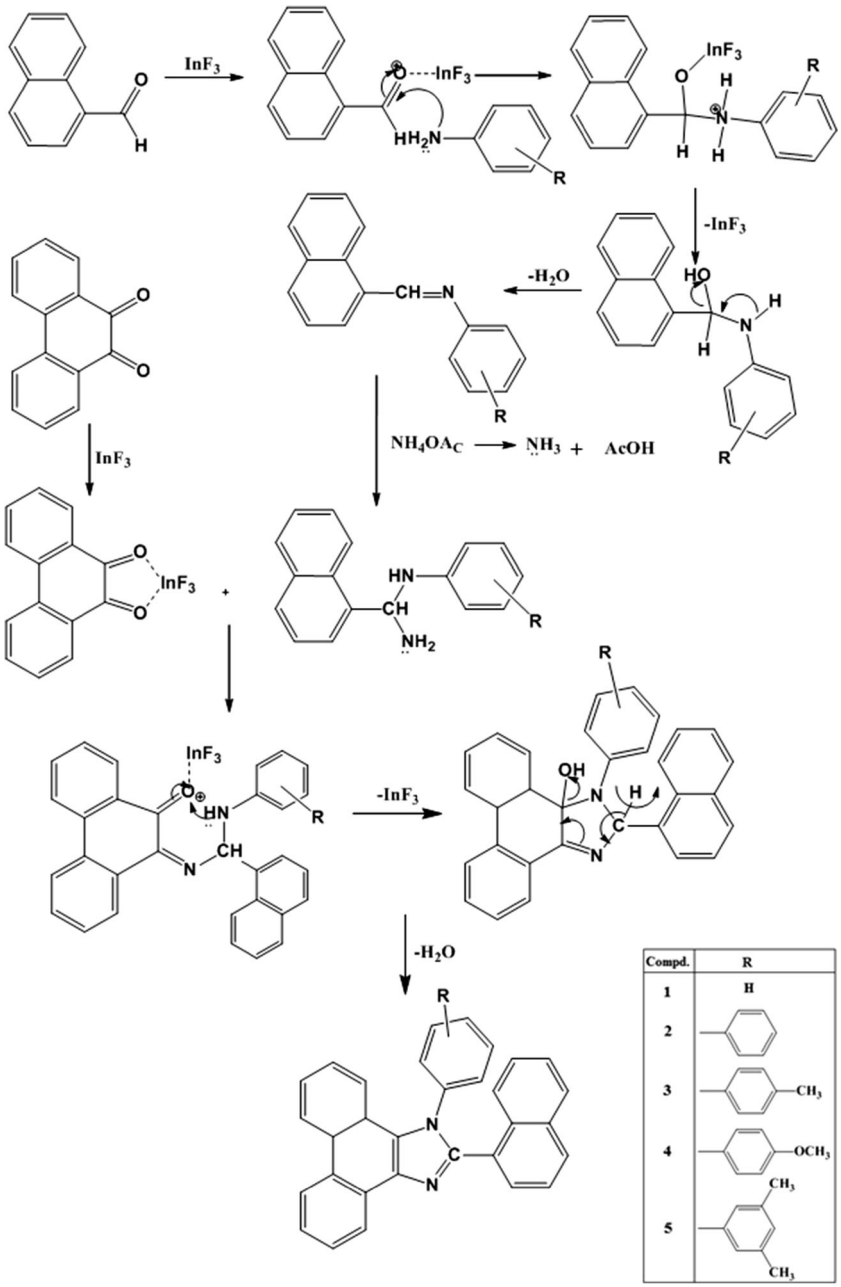

related to the electronic interactions between the remaining pairs of atoms in the D–A molecule (this contribution is usually small and negligible) . Expressions 2 and 3 assume that the ^{1}LE state is mainly described by a configuration corresponding to the HOMO→LUMO excitation (e.g., ^1L_a state in Platt's notation). Here, we report the synthesis, characterisation and solvatochromism of newly synthesized π– expanded imidazole derivatives. The influence of solvents on the photophysical properties of the imidazole derivatives with solvent polarity function have been discussed in terms of absorption, emission, dipole moments, change in free energy and reorganisation energy.

Experimental

Chemicals

1-naphthaldehyde and phenanthrene-9,10-dione were supplied by Sigma-aldrich (St.Louis, USA). Aniline, 4-methylaniline, 4-methoxyaniline and 3,5-dimethylaniline

were used of analytical grade and received from S.D. Fine (Mumbai, India). The solvents used were of spectroscopic grade supplied by Himedia (Chennai, India).

Spectral Measurements

The proton and proton decoupled ^{13}C NMR spectra were recorded using a Bruker 400 MHz NMR spectrometer (Bruker biospin, California, USA) operating at 400 MHz and 100 MHz, respectively. The mass spectra of the samples were obtained using a Thermo Fischer LC-Mass spectrometer in FAB mode. The UV–vis absorption and fluorescence spectra were recorded with PerkinElmer Lambda 35 spectrophotometer and PerkinElmer LS55 spectrofluorimeter, respectively.

Computational Details

The quantum chemical calculations were carried out using the Gaussian 03 [24] package. Optimization and HOMO—LUMO frontier orbital of phenanthrimidazole derivatives were performed using density functional theory (DFT).

Synthesis of Polysubstituted Phenanthrimidazoles

A mixture of naphthaldehyde (1 mmol), phenanthrene-9,10-dione (1 mmol), aniline (1 mmol), ammonium acetate (1 mmol) and InF_3 (1 mol%) was stirred at 80 °C and the progress of the reaction was monitored by TLC. After completion of the reaction, the mixture was cooled, dissolved in acetone and filtered. The product was purified by column chromatography using benzene: ethyl acetate (9:1) as the eluent (Scheme 1). The newly synthesised phenanthrimidazoles have been characterised by CHN analysis, ^1H and ^{13}C NMR and mass spectra.

2-(Naphthalen-1-yl)-1H-Phenanthro[9,10-d]Imidazole *(1)*

M.p. 262 °C., Anal. calcd. for $C_{25}H_{16}N_2$: C, 87.18; H, 4.68; N, 8.13. Found: C, 87.16; H, 4.67; N, 8.12. ^1H NMR (400 MHz, DMSO): δ 10.41 (s, 1H), 7.37 (s, 4H), 8.77 (d, *J*=7.2 Hz, 3H), 7.90 (d, *J*=8.0 Hz, 2H), 7.82 (d, *J*=7.2 Hz,1H), 7.66 (t, 4H), 7.54–7.45 (m, 3H). ^{13}C NMR (400 MHz, $CDCl_3$): δ 121.83, 123.78, 124.97, 125.47, 125.89, 126.38, 127.12, 127.29, 127.58, 127.88, 128.37, 128.47, 130.16, 131.30, 133.92, 148.87. MS: m/z. 344 [M+].

2-(Naphthalen-1-yl)-1-Phenyl-1H-Phenanthro[9,10-d] Imidazole *(2)*

M.p. 265 °C., Anal. calcd. for $C_{31}H_{20}N_2$: C, 88.54; H, 4.79; N, 6.66. Found: C, 88.52; H, 4.78; N, 6.65. ^1H NMR (400 MHz, DMSO): δ 8.89 (d, *J*=7.6 Hz, 1H), 8.80 (d, *J*=8.4 Hz, 1H), 8.75 (d, *J*=7.6 Hz, 1H), 7.99 (d, *J*=5.6 Hz, 1H),7.83 (d, *J*=7.6 Hz, 2H), 7.74 (t, 1H), 7.67 (t, 1H), 7.53 (t, 1H), 7.48–7.43 (m, 3H), 7.35–7.29 (m, 6H). ^{13}C NMR (400 MHz, $CDCl_3$): δ 121.07, 122.89, 123.01, 123.18, 124.16, 124.48, 125.02, 125.65, 126.02, 126.17, 126.34, 126.88, 127.38, 127.44, 128.05, 128.15, 128.34, 128.49, 129.28, 129.48, 129.55, 129.73, 133.21, 133.47, 137.38, 138.04, 150.48. MS: m/z. 420 [M+].

2-(Naphthalen-1-yl)-1-p-Tolyl-1H-Phenanthro[9,10-d] Imidazole *(3)*

M.p. 248 °C., Anal. calcd. for $C_{32}H_{22}N_2$: C, 88.45; H, 5.10; N, 6.45. Found: C, 88.41; H, 5.07; N, 6.42. ^1H NMR (400 MHz, DMSO): δ 2.32 (s, 3H), 8.88 (d, *J*=7.6 Hz, 1H), 8.79 (d, *J*=8.4 Hz, 1H), 8.73 (d, *J*=8.0 Hz, 1H), 7.96 (d, *J*=7.2 Hz, 1H), 7.80 (d, *J*=8.0 Hz, 2H), 7.20 (d, *J*=7.6 Hz, 2H), 7.10 (d, *J*=8.0 Hz, 2H), 7.71 (t, 1H), 7.65 (t, 1H), 7.53 (t, 1H), 7.43 (q, 3H) 7.35–7.24 (m, 4H). ^{13}C NMR (400 MHz, DMSO): δ 21.31, 121.11, 122.87, 123.12, 123.20, 124.14, 124.50, 124.70, 125.00, 125.10, 125.62, 126.04, 126.14, 126.35, 126.83, 127.38, 127.53, 127.77, 128.15, 128.34, 128.39, 129.28, 129.47, 129.67, 130.20, 133.23, 133.44, 133.76, 135.32, 137.27, 139.29, 150.63. MS: m/z. 434 [M+].

1-(4-Methoxyphenyl)-2-(Naphthalen-1-yl) -1H-Phenanthro[9,10-d]Imidazole *(4)*

M.p. 272 °C., Anal. calcd. for $C_{32}H_{22}N_2O$: C, 85.31; H, 4.92; N, 6.22; O, 3.55. Found: C, 85.30; H, 4.91; N, 6.21; O, 3.54. ^1H NMR (400 MHz, DMSO): δ 3.72 (s, 3H), 8.96 (d, *J*=8.4 Hz, 1H), 8.91 (d, *J*=8.4 Hz, 1H), 8.66 (d, *J*=7.6 Hz, 1H), 7.89 (d, *J*=8.0 Hz, 1H), 7.76 (d, *J*=7.2 Hz, 1H), 7.57 (d, *J*=7.6 Hz, 1H), 7.38 (t, 1H), 7.20 (d, *J*=8.0 Hz, 1H), 6.94 (d, *J*=8.4 Hz, 2H), 7.96 (t, 2H), 7.69(t, 2H), 7.55–7.42 (m, 5H). ^{13}C NMR (400 MHz, DMSO): δ 55.28, 114.62, 120.27, 121.98, 122.59, 123.66, 124.42, 124.67, 125.19, 125.60, 125.78, 126.20, 126.69, 126.82, 126.86, 127.24, 127.42, 127.64, 128.04, 128.09, 128.29, 128.41, 129.50, 129.52, 129.72, 129.95, 132.35, 132.76, 136.28, 150.47, 159.47. m/z. 450 [M+].

1-(3,5-Dimethylphenyl)-2-(Naphthalen-1-yl) -1H-Phenanthro[9,10-d]Imidazole *(5)*

M.p. 261 °C., Anal. calcd. for $C_{33}H_{24}N_2$: C, 88.36; H, 5.39; N, 6.25. Found: C, 88.35; H, 5.38; N, 6.24. ^1H NMR (400 MHz, DMSO): δ 2.17 (s, 6H), 8.96 (d, *J*=8.0 Hz, 1H), 8.91 (d, *J*=8.0 Hz, 1H), 8.64 (d, *J*=7.6 Hz, 1H), 7.97 (t, 2H), 7.91 (d, *J*=7.2 Hz, 1H), 7.76 (d, *J*=7.2 Hz, 1H), 7.74 (d, *J*=6.4 Hz, 2H), 7.08 (s, 1H), 7.16 (t, 2H), 7.36–7.40 (m, 3H),7.60–7.48 (m, 3H). ^{13}C NMR (400 MHz, DMSO): δ 20.54, 120.36, 121.99, 122.45, 123.66, 124.42, 124.66, 125.22, 125.44, 125.66, 125.83, 126.06, 126.22, 126.33, 126.71, 126.76, 127.00, 127.23, 127.45, 127.62, 127.90, 128.04, 128.29, 128.40,

129.54, 131.01, 132.28, 132.75, 136.27, 137.28, 138.90, 150.06. MS: m/z. 448 [M+].

Result and Discussion

Catalytic Activity of Indium Trifluoride

Initially, the condensation reaction was carried out in the presence of InF_3 (1 mol%), naphthaldehyde (1 mmol), ammonium acetate (1 mmol), and arylamine (1 mmol) in different solvents such as water, ethanol, methanol, chloroform, and acetonitrile under refluxing and also in solvent-free conditions at 80 °C (Scheme—1). From observation made from above experiments the solvent-free condition is taken as the best for imidazole synthesis. In the absence of catalyst under solvent-free conditions at room temperature the yield is very poor even after 24 h. To improve the yield of the product, the temperature was increased to 200 °C, but no appreciable increment was observed. We found that presence of a catalytic amount of InF_3 under solvent-free condition is the best for this synthesis; maximum yield (76 %) was obtained at 36 min on loading with 1 mol% of InF_3 at 80 °C (Table 1). Moreover, InF_3 can be recovered and reused several times without significant loss of activity. High product yield, shorter reaction time, low catalyst loading and easy work-up procedure, make this procedure quite simple and more convenient. Our methodology could be a valid contribution to the existing processes of imidazole synthesis.

Table 1 Effect of catalyst and temperature in the synthesis of phenanthrimidazole derivatives

Entry	Temp (°C)	Solvent	InF_3		InF_3 (mol%)
			Time (min)	Yield (%)	
1	r.t	Solvent-free	135 (385)	65(Trace)	0.1
2	50	Solvent-free	68(266)	62(20)	0.1
3	70	Solvent-free	32(89)	68(45)	0.1
4	90	Solvent-free	28(100)	70(52)	0.1
5	80	Solvent-free	36	76	1
6	80	Solvent-free	28	79	2
7	80	Solvent-free	47	80	10
8	80	Water	100	32	1
9	80	Ethanol	45	60	1
10	80	Methanol	55	65	1
11	80	Chloroform	146	46	1
12	80	Acetonitrile	90	62	1

values in the parentheses corresponds to absence of catalyst

Absorption and Fluorescence Spectra

Room temperature absorption spectra of 2-naphthylphenanthrimidazoles in n-hexane are shown in Fig. 1. The superposition of the bands observed corresponding to the donor and acceptor subunits which seem to be only slightly perturbed by their interactions. The first three absorption bands of are assigned to $^1(\pi\text{-}\pi^*)$ states correspond in Platt's notation to the ^1L_b, ^1L_a and ^1B_a excited states. The low and high energy transitions $^1L_b \leftarrow S_0$, $^1L_a \leftarrow S_0$ and $^1B_a \leftarrow S_0$ respectively, observed in the absorption spectra of all compounds studied [25, 26]. The low energy absorption region of the D-A phenanthrimidazole derivatives containing naphthyl as an electron acceptor indicates the presence of charge transfer states [27]. Assuming a point dipole situated in the center of the spherical cavity and neglecting the mean solute polarizability in the states involved in the transition it follows [28–31],

$$hc\tilde{\upsilon}^{vac}_{abs\,abs\approx} hc\tilde{\upsilon}^{vac}_{abs} - 2\mu_g(\mu_e - \mu_g)/a_o^3\left[(\varepsilon-1)/(2\varepsilon+1) - {}^1/_2(n^2-1)/(2n^2+1)\right] \quad (4)$$

where μ_g and μ_e are dipole moments of the solute in the ground and excited states, respectively, $_{abs}$ and $\tilde{\upsilon}^{vac}_{abs}$ are the spectral positions of a solvent-equilibrated absorption maxima and the value extrapolated to the gas-phase, respectively, a_o is the effective radius of the Onsager cavity [32, 33] and ε and n are the static dielectric constant and the refractive index of the solvent, respectively. Equation 4 is used to determine the values of μ_g $(\mu_e - \mu_g) / a_o^3$ and $\tilde{\upsilon}^{vac}_{abs}$ (Fig. 2a). The blue shift of the CT absorption bands indicate the dipole molecule cannot be approximated by the point dipole situated in the center of the cavity (Fig. 2b). The ground state dipole moment is determined by polar groups lying far from the center of the molecule which leads to an increase of the effective Onsager reaction field [10, 28] and increase the ground state salvation energies. Therefore blue shift is observed in the absorption spectra for the presently studied molecules.

In the excited state, the negative and positive ends of the electric dipole are localized nearly in the centres of the donor and acceptor fragments, respectively. The observed red shift and increase of Stokes shift with increasing solvent polarity in fluorescence spectra with excitation wavelength 260 nm point to the CT character of the fluorescent states. The excited state dipole moments μ_e estimated by the fluorescence solvatochromic shift method imply the excited states live sufficiently long with respect to the orientation relaxation time of the solvent [34–36]. Under the same assumption as used for above expression, it follows that,

$$hc\tilde{\upsilon}_{flu\approx} hc\tilde{\upsilon}^{vac}_{flu} - 2\mu_e(\mu_e - \mu_g)\Big/a_o^3\Big[(\varepsilon-1)\Big/(2\varepsilon+1) - {}^1/_2(n^2-1)\Big/(2n^2+1)\Big] \quad (5)$$

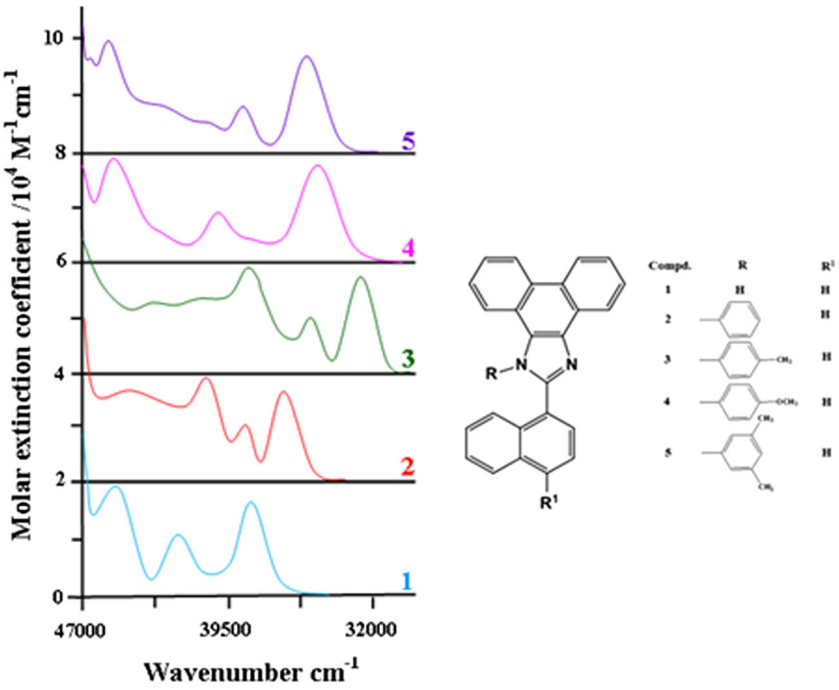

Fig. 1 Absorption spectra of donor-acceptor phenanthrimidazoles 1–5

where $_{flu}$ and $vkern - 6ptvskip - 7.5pt\tilde{}^{vac}_{flu}$ are the spectral positions of the solvent equilibrated fluorescence maxima and the value extrapolated to the gas-phase, respectively. There is a linear correlation between the energy (hc $_{flu}$) and the solvent polarity function in a polar environment and also in all solvents (Fig. 2c). The values of μ_e (μ_e - μ_g) / a_o^3 extracted from the data measured in polar media are somewhat larger than whole range of the solvents. The observed red shift dependence upon the electronic structure of the fluorescent states on solvation. In nonpolar solvents due to a relatively small energy gap between the lowest CT states and the locally excited states reveal that an increasing contribution of π, π * character to the wave function of the CT states. This leads to lowering of energy by stabilizing such interactions and results red shift in the fluorescence spectra. The quantity (μ_e - μ_g) ^{2} / a_o^3 can be evaluated from the solvation effects on Stokes shift by using the following expression,

$$hc(\tilde{\upsilon}_{abs}-\tilde{\upsilon}_{flu}) = hc\left(\tilde{\upsilon}^{vac}_{abs}-\tilde{\upsilon}^{vac}_{flu}\right) + 2(\mu_e-\mu_g)^2/a_o^3\left[(\varepsilon-1)/(2\,\varepsilon+1)-{}^1\!/_2\,(n^2-1)/(2n^2+1)\right] \quad (6)$$

(6)

There is a linear correlation between energy (hc_{abs} - hc_{flu}) and solvent polarity function in a polar environment and also in all solvents studied (Fig. 3a), the values of (μ_e - μ_g)^2 / a_o^3 are, 0.82 eV (1), 0.91 eV (2), 1.09 eV (3), 1.26 eV (4) and 1.31 eV (5). Under the assumption that $\mu_e >> \mu_g$ and with the effective spherical radius (a_0) of the molecules, 5.61 A° (1), 6.00 A° (2), 6.08 A° (3), 6.15 A° (4) and 6.99 A° (5) (calculated by molecular mechanics), Eqs. 5 and 6 yield very similar values of μ_e as 13.25 D (1), 14.98 D (2), 15.86 D (3), 17.85 D (4) and 25.84 D (5). The large value of $\Delta\mu = \mu_e - \mu_g \approx 8.68$ D (1), 11.24 D (2), 17.29 D (3), 18.56 D (4) and 20.21 D (5) corresponds to a charge separation of range 0.3–0.6 nm which roughly agrees with centre-to-centre distance between donor and acceptor moieties and indicates the full electron transfer takes place in all D- A systems studied.

According to Marcus [37], E (A)=$\Delta G_{solv}+\lambda_1$ and E (F)= ΔG_{solv} - λ_0, where E(A) and E(F) are absorption and fluorescence band maxima in cm,$^{-1}$ respectively, ΔG_{solv} is difference in free energy of the ground and excited states in a given solvent and λ represents the reorganization energy. The free energy changes of solvation and reorganization energies in

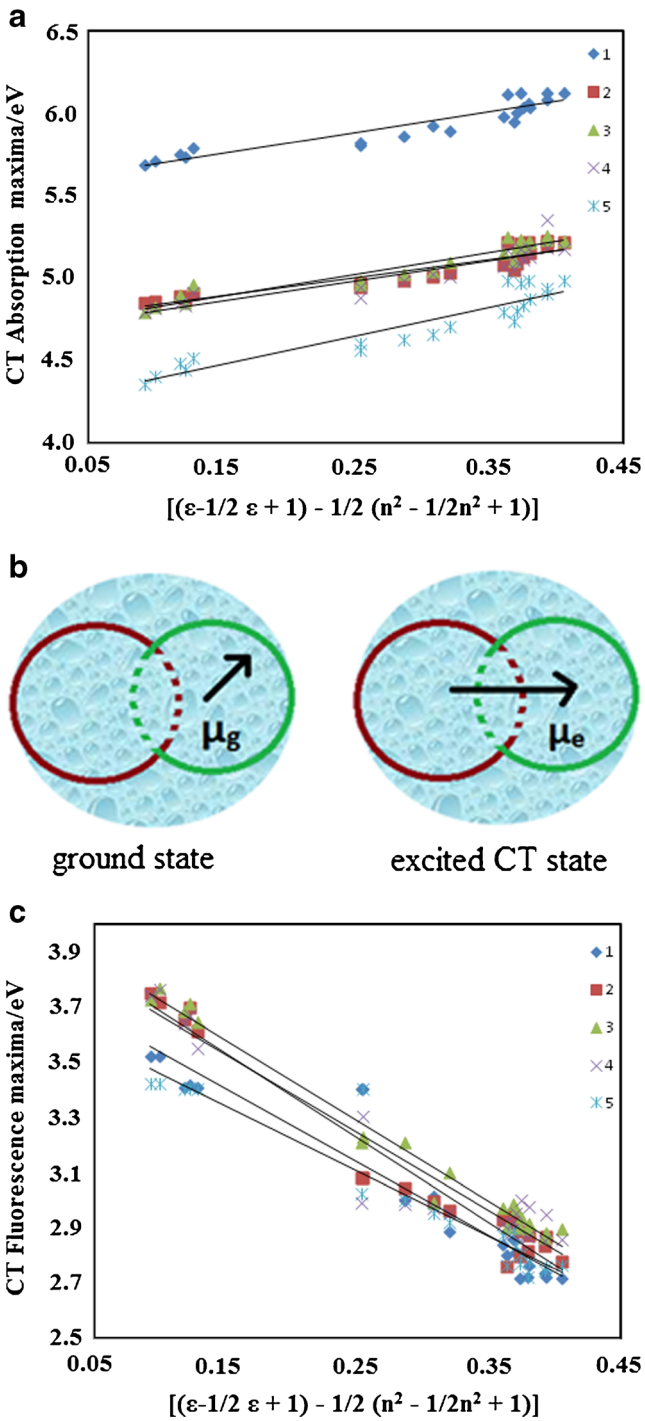

Fig. 2 **a** Solvatochromic shift of energy related to CT absorption maxima as a function of solvent polarity function; **b** Dipolemoments direction in ground and excited states; **c** Solvatochromic shift of energy related to CT fluorescence maxima as a function of solvent polarity function

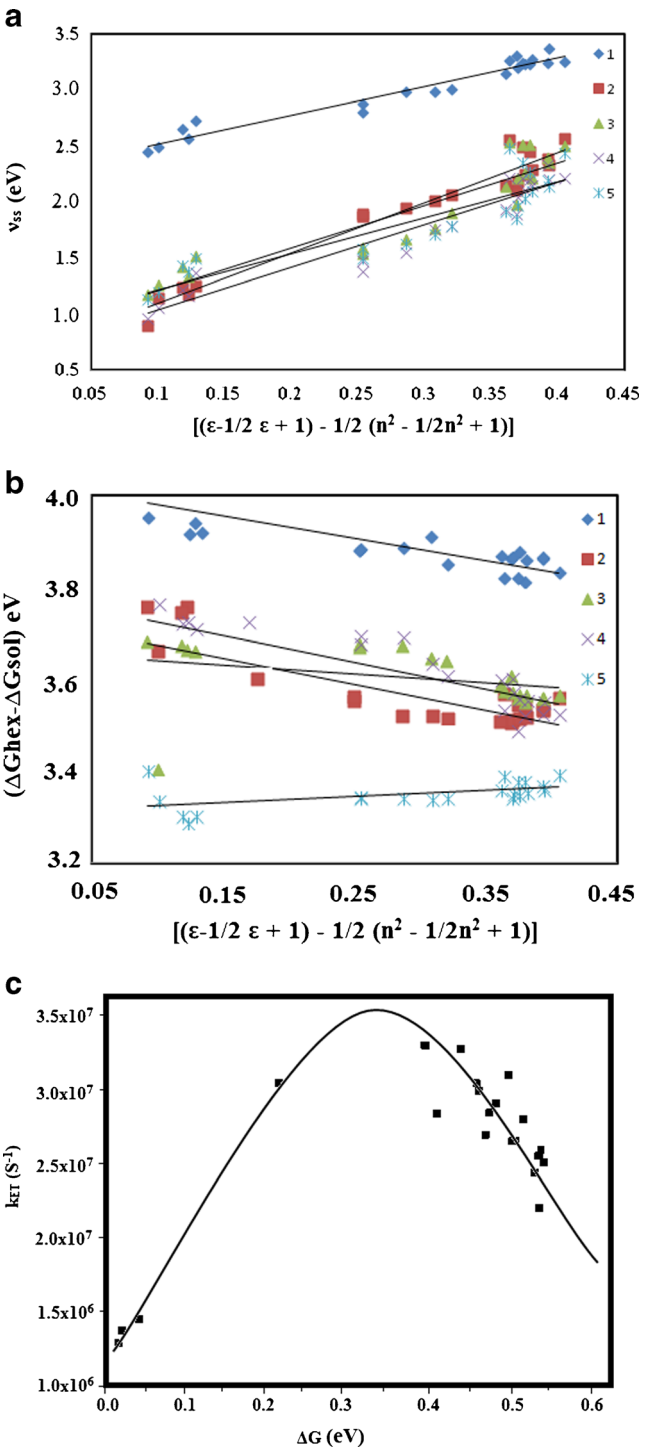

Fig. 3 **a** Solvatochromic shift of energy related to Stokes shift as a function of solvent polarity parameter; **b** Plot of free energy change ΔG versus solvent polarity function of each solvent; **c** Plot of rate constant k_{ET} against change in free energy

various solvents have been estimated. Under the assumption that $\lambda_0 \approx \lambda_1 \approx \lambda$, E (A)+E (F)=2$\Delta G_{solv}$; E (A) - E (F)=2 λ. The ΔG_{solv} is maximum for hexane and minimum in water and the difference between these values give the free energy change required for hydrogen bond formation. The plot of $\Delta G_{solv}=(\Delta G_{hex} - \Delta G_{water})$ versus solvent polarity function has been depicted in Fig. 3b [38]. In aprotic solvents the values are small and interaction of phenanthrimidazole derivatives with those solvents is purely due to dipolar interactions

a

Compd.	HOMO	LUMO	HOMO-1	LUMO+1
1				
2				
3				
4				
5				

b

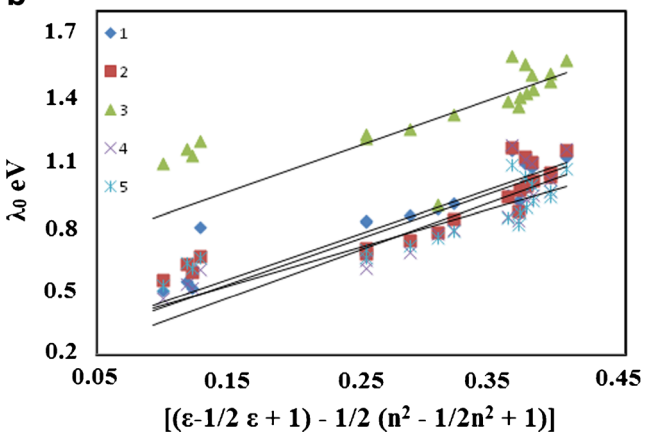

Fig. 4 **a** HOMO-LUMO orbitals contour map; **b** Correlation between reorganisation energy (λ_0) depend on the solvent polarity function

in the excited state. The definite values of reorganization energy confirmed the interaction between solvent and solute. The electronic coupling interaction between donor and acceptor fragments through the intervening σ-bond has been explained by Turro et al., [39]. The rate constant (k_{ET}) for electron transfer has been calculated using the equation, k_{ET} $= (1/\tau)(\lambda_0/16\pi RT)^{1/2} \exp(-\lambda_0/4RT)$ [40, 41]. The rate constant (k_{ET}) plotted against the change in free energy is shown in Fig. 3c which reveal an initial rise of the rate with increasing free energy change followed by an inverted region where further increases of the driving force leads to a decrease in rate.

The wave function of spectroscopic CT state is a linear combination of zero-order ET state (^{1}ET) with various locally excited $^1(\pi, \pi^*)$ states (L_a^1 and L_b^1 states of the donor moieties due to low energy) and with ground state (S_0) [42],

$$\psi_{CT}^1 \cong C_{ET}\Phi_{ET}^1 + C_a\Phi_{La}^1 + C_b\Phi_{Lb}^1 + C_0\Phi_{s0}^1 \quad (7)$$

where Φ_{s0}^1, Φ_{ET}^1, Φ_{La}^1 and Φ_{Lb}^1 represent the closed-shell configuration of ground state, zero-order wave functions of pure ^{1}ET state and L_a^1 and L_b^1 states of the donor moieties, respectively. The ^{1}ET state indicates electron transfer from HOMO orbital of the donor to LUMO orbital of the acceptor. The frontier molecular orbital diagram (Fig. 4a) shows the HOMO electron density is localised on the phenanthrimidazole moiety and the LUMO electron density is localised on the naphthyl fragment and also imply that there is a charge transfer from HOMO to LUMO orbitals. The obtained Δμ, 8.68 D (1), 11.24 D (2), 17.29 D (3), 18.56 D (4) and 20.21 D (5) suggest that the wave functions (ψ_{CT}^1) of the ^{1}CT states are in the order 5>4>3>2>1. The value of $hc\tilde{\upsilon}_{abs}^{vac}$ is also following the same trend which is due to mixing of the lowest pure ^{1}ET state with $^1(\pi, \pi^*)$ excitation leads to lowering ^{1}CT energy due to a stabilisation of such interactions. It is also in agreement with the magnitude of electronic coupling elements V_1^D estimated from Eq. 3 reveal the contribution of $^1(\pi, \pi^*)$ character to the wave function ψ_{CT}^1 should decrease in the order of 5>4>3>2>1.

The reorganisation energy (λ_0) is related to low-frequency motions such as reorientation of the solvent shell (λ_s) as well as any other low-frequency and medium frequency nuclear motions of the solute ($\delta\lambda_0$). The inner reorganization energy (λ_i) corresponds to high-frequency motion associated with changes in the solute bond length and angle. The low-frequency reorganization energy (λ_0) depend on solvent polarity (Fig. 4b) shown by the following expression:

Table 2 Slopes and intercepts of the solvatochromic plots of the CT fluorescence of the phenanthrimidazoles (1–5)

Compd.	Nonpolar solvents and polar solvents				Polar solvents only		Nonpolar solvents and polar solvents
	$\Delta\mu$ (D)	μ_e (D)	$hc\,\tilde{U}_{flu}^{vac}$, eV	$\mu_e(\mu_e - \mu_g)/a_o^3$ eV	$hc\,\tilde{U}_{flu}^{vac}$, eV	$\mu_e(\mu_e - \mu_g)/a_o^3$ eV	$(\mu_e - \mu_g)^2/a_o^3$ eV
1	8.68	13.25	3.19	0.82	3.30	1.00	1.00
2	11.24	14.98	3.21	0.91	3.42	1.15	1.30
3	17.29	15.86	3.23	1.09	3.46	1.29	1.32
4	18.56	17.85	3.25	1.26	3.49	2.34	1.40
5	20.21	25.84	3.62	1.31	3.80	1.42	1.43

$$\lambda_{0\approx}\delta\lambda_{0+}\lambda_{0\approx}\delta\lambda_{0+}\left(\mu_e-\mu_g\right)^2/a_o^3\left[(\varepsilon-1)/(2\,\varepsilon\,+1)-{}^1/_2\left(n^2-1\right)/\left(2n^2+1\right)\right] \quad (8)$$

The values of $(\mu_e - \mu_g)^2 / a_o^3$ [(1.00 eV (1), 1.30 eV (2), 1.32 eV (3), 1.40 eV (4) and 1.43 eV (5)] obtained from the slope of the plots agree with those displayed in Table 2. This finding also supports that the wave functions (ψ_{CT}^1) of the ^{1}CT states are in the order of 5>4>3>2>1 and also the conformation of the emitting ^{1}CT states does not differ remarkably from that in the ground state.

Conclusions

Photo induced intramolecular charge transfer states of selected D–A derivatives of phenanthrimidazole containing naphthyl as an electron acceptor has been analysed by electronic spectra. Relatively small energy gap between the lowest CT states and the locally excited states reveal that an increasing contribution of π, π * character to the wave function of the CT states. This leads to lowering of energy by stabilizing such interactions and results red shift in the fluorescence spectra. The $(\mu_e - \mu_g)^2 / a_o^3$ are, 0.82 eV (1), 0.91 eV (2), 1.09 eV (3), 1.26 eV (4) and 1.31 eV (5) calculated from the linear correlation between energy ($hc_{abs} - hc_{flu}$) and solvent polarity function. The electronic coupling element (V_0) calculated by using $\Delta\mu=\mu_e - \mu_g\approx$8.68 D (1), 11.24 D (2), 17.29 D (3), 18.56 D (4) and 20.21 D (5) gives information that the conformation of the emitting ^{1}CT states does not differ from that in the ground state. The calculated free energy change indicates the electron transfer is in the inverted Marcus region.

Acknowledgments One of the authors Prof. J. Jayabharathi is thankful to DST [No. SR/S1/IC-73/2010], DRDO (NRB-213/MAT/10-11), UGC (F. No. 36-21/2008 (SR)) and CSIR (NO 3732/NS-EMRII) for providing funds to this research study.

References

1. Hush NS (1985) Distance dependence of electron transfer rates. Coord Chem Rev 64:135–157
2. Marcus RA (1989) Relation between charge transfer absorption and fluorescence spectra and the inverted region. J Phys Chem 93: 3078–3086
3. Gould IR, Young RH, Moody RE, Farid S (1991) Contact and solvent-separated geminate radical ion pairs in electron-transfer photochemistry. J Phys Chem 95:2068–2080
4. Gould IR, Noukakis D, Gomez-Jahn L, Young RH, Goodman JL, Farid S (1993) Radiative and nonradiative electron transfer in contact radical-Ion pairs. J Chem Phys 176:439–456
5. Cortes J, Heitele H, Jortner J (1994) Band shape analysis of the charge transfer fluorescence in barrelene based electron-donor-acceptor compounds. J Phys Chem 98:2527–2536
6. Mulliken RS, Person WB (1969) Molecular complexes: a lecture and reprint volume. Weinheim, VCH
7. Murrell JN (1959) Molecular complexes and their spectra. IX the relationship between the stability of a complex and the intensity of its charge-transfer bands. J Am Chem Soc 81:5037–5043
8. Bixon M, Jortner J, Verhoeven JW (1994) Lifetimes for radiative charge recombination in donor-acceptor molecules. J Am Chem Soc 116:7349–7355
9. Herbich J, Kapturkiewicz A (1998) Electronic structure and molecular conformation in the excited charge transfer singlet states of p-acridyl and other aryl derivatives of aromatic amines. J Am Chem Soc 120:1014–1029
10. Kapturkiewicz A, Herbich J, Karpiuk J, Nowacki J (1997) Intramolecular radiative and radiationless charge recombinations in donor-acceptor carbazole derivatives. J Phys Chem A 101: 2332–2344
11. Kapturkiewicz A, Nowacki J (1999) Properties of the intramolecular excited charge-transfer states of carbazol-9-yl derivatives of aromatic ketones. J Phys Chem A 103:8145–8155
12. Borowicz P, Herbich J, Kapturkiewicz A, Nowacki J (1999) Excited charge-transfer states in donor-acceptor indole derivatives. Chem Phys 244:251–261
13. Borowicz P, Herbich J, Kapturkiewicz A, Nowacki J, Opallo M (1999) Radiative and nonradiative electron transfer in donor-acceptor phenoxazine and phenothiazine derivatives. Chem Phys 249:49–62
14. Grabowski ZR, Rotkiewicz K, Siemiarczuk A, Cow-ley DJ, Baumann W (1979) Nouv. Twisted intramolecular charge transfer states (TICT). A new class of excited states with a full charge separation. J Chim 3:443–454
15. Masaki S, Okada T, Mataga N, Sakata Y, Misumi S (1976) On the solvent-induced changes of electronic structures of intramolecular exciplexes. Bull Chem Soc Jpn 49:1277–1283
16. Richard JP, Amyes TL (2001) Proton transfer at carbon. Curr Opin Chem Biol 5:626–633
17. Stoner Ma D, Jaye AA, Ronayne KL, Nappa J, Meech SR, Tonge PJ (2008) An Alternate proton acceptor for excited state protein transfer in green fluorescent protein: rewiring GFP. J Am Chem Soc 130: 1227–1235
18. Paterson MJ, Robb MA, Blancafort L, DeBellis AD (2005) Mechanism of an exceptional class of photostabilizers: a seam of conical intersection parallel to excited state intramolecular proton transfer (ESIPT) in o-hydroxyphenyl-(1,3,5)-triazine. J Phys Chem A 109:7527–7537
19. Lim SJ, Seo J, Park SY (2006) Photochromic switching of excited-state intramolecular proton-transfer (ESIPT) fluorescence: a unique route to high-contrast memory switching and nondestructive readout. J Am Chem Soc 128:14542–14547
20. Klymchenko AS, Shvadchak VV, Yuschenko DA, Jain N, Mély Y (2008) Excited-state intramolecular proton transfer distinguishes microenvironments in single- and double-stranded DNA. J Phys Chem B 112:12050–12055
21. Kwon JE, Park SY (2011) Advanced Organic optoelectronic materials: harnessing excited-state intramolecular proton transfer (ESIPT) process. Adv Mater 23:3615–3642
22. Dogonadze RR, Kuznetsov AM, Marsagishvili TA (1980) The present state of the theory of charge transfer in condensed phase. Electrochim Acta 25:1–28
23. Mataga N, Kaifu Y, Koizumi M (1955) The solvent effect on fluorescence spectrum. Change of solute-solvent interaction during the lifetime of excited solute molecule. Bull Chem Soc Jpn 28:690
24. Frisch MJ, Trucks GW, Schlegel HB, Scuseria GE, Robb MA, Cheeseman JR, Montgomery JA Jr, Vreven T, Kudin KN, Burant JC, Millam JM, Iyengar SS, Tomasi J, Barone V, Mennucci B, Cossi M, Scalmani G, Rega N, Petersson GA, Nakatsuji H, Hada M, Ehara M, Toyota K, Fukuda R, Hasegawa J, Ishida M, Nakajima T, Honda

Y, Kitao O, Nakai H, Klene M, Li X, Knox JE, Hratchian HP, Cross JB, Bakken V, Adamo C, Jaramillo J, Gomperts R, Stratmann RE, Yazyev O, Austin AJ, Cammi R, Pomelli C, Ochterski JW, Ayala PY, Morokuma K, Voth GA, Salvador P, Dannenberg JJ, Zakrzewski VG, Dapprich S, Daniels AD, Strain MC, Farkas O, Malick DK, Rabuck AD, Raghavachari K, Foresman JB, Ortiz JV, Cui Q, Baboul AG, Clifford S, Cioslowski J, Stefanov BB, Liu G, Liashenko A, Piskorz P, Komaromi I, Martin RL, Fox DJ, Keith T, Al-Laham MA, Peng CY, Nanayakkara A, Challacombe M, Gill PMW, Johnson B, Chen W, Wong MW, Gonzalez C, Pople JA (2004) Gaussian 03 (Revision E.01). Gaussian, Inc, Wallingford

25. Chiba K, Aihara JI, Araya K, Matsunaga Y (1980) The Electronic spectra of intramolecular charge-transfer compounds and their marked solvatochromism in a strong hydrogen-bonding solvent: 2-(arylmethylene)-1,3-indandiones and 2-(1-naphthyl)-*p*-benzoquinone. Bull Chem Soc Jpn 53: 1703–1708
26. McGlynn SP, Azumi T, Kinoshita M (1969) Molecular spectroscopy of the triplet state. Prentice Hall, Englewood Cliffs
27. Willard DM, Riter RE, Levinger NE (1998) Dynamics of polar solvation in lecithin/water/cyclohexane reverse micelles. J Am Chem Soc 120:4151–4160
28. Bottcher CJF, Van Belle OC, Bordewijk P, Rip A (1973) In theory of electronic polarization, Eeds. Elsevier, Amsterdam, Vol. I
29. Czerwieniec R, Herbich J, Kapturkiewicz A, Nowacki J (2000) Radiative electron transfer in planar donor–acceptor quinoxaline derivatives. Chem Phys Lett 325:589–598
30. Jayabharathi J, Thanikachalam V, Sathishkumar R (2014) Excited charge transfer states in donor–acceptor fluorescent phenanthroimidazole derivatives. J Fluoresc 24:431–444
31. Liptay W, Lim EC (1974) Polarizabilities of molecules in excited electronic state. In: In Excited States, Ed. Academic, New York, p 129
32. Rettig W, Zander M (1982) On Twisted intramolecular charge transfer (TICT) stated in N-aryl-carbazoles. Chem Phys Lett 87:229–234
33. Onsager L (1936) Electric moments of molecules in liquids. J Am Chem Soc 58:1486–1493
34. Bo¨ttcher CJF, Van Belle OC, Bordewijk P, Rip A (1973) In Theory of electric polarization, Eds. Elsevier, Amsterdam, Vol. I
35. Lippert EZ (1955) Dipolmoment and Elektronenstruktur von angeregten Molekülen. Naturforsch 10:541–545
36. Mataga N, Kaifu Y, Koizumi M (1956) On the base strength of some nitrogen heterocycles in the excited state. Bull Chem Soc Jpn 29: 373–379
37. McRae EG (1957) Theory of solvent effects on molecular electronic spectra. Frequency shifts. J Phys Chem 61:562–572
38. Marcus RA (1963) Free Energy of nonequilibrium polarization systems. II. Homogeneous and electrode systems. J Chem Phys 38:1858
39. Castellan GW (1985) Physical chemistry, 3rd edn. Narosa Publishing House, Delhi
40. N.J. Turro, V. Ramamurthy and J.C. Scaiano, (2009), Principles of Molecular Photochemistry: An introduction, University Science books
41. Kapturkiewicz A (1992) Electrochemical generation of excited TICT states. V. Evidence of inverted Marcus region. J Chem Phys 166:259
42. Mulliken RS (1952) Molecular compounds and their spectra. J Am Chem Soc 74:811–824